

High Precision Color Management by Polar Coordinate Division in CIELAB Space

Atsumi Ishige, Hiroaki Kotera and Chen Hung-Shing
Department of Information and Image Sciences, Chiba University

Abstract

A variety of color calibration technologies has been developed for input/output devices. Linear or nonlinear matrices have been conveniently applied to correct the color filter's mismatch in scanner or suppress the cross talks of colorants in printer. The color matching errors are furthermore reduced when the nonlinear matrices are optimized in subdivided smaller spaces than in an entire color space. This paper proposes a new method for partitioning the color space into subspaces to improve the accuracy. Linear or nonlinear color correction functions are applied to each subspace and the matrices are optimized individually. The new method resulted in the high precision color matchings with rms color differences ΔE_{ab}^* (rms) ≤ 0.5 for flat bed scanner and ΔE_{ab}^* (rms) $\cong 2.0$ for inkjet printer. The accuracies are approaching to the measurement errors in scanner and mechanical stabilities in printer.

Introduction

The color management is a key technology to reproduce the accurate colors across the different media. The color signals from input devices should be calibrated to carry the correct tristimulus values and the color masking process is indispensable for printer or copier to eliminate the cross talks in colorants. Linear and nonlinear correction matrices have been conveniently applied to reduce the colorimetric errors in scanner^{3,5,7} or printer^{1,4,6,8}. The accuracy can be furthermore improved when the matrices or look-up tables in device profiles are optimized in subdivided spaces than in entire space^{2,9}.

This paper discusses the partitioning method of input color space into subspaces, where the equal number of the color samples are included in every subspaces to determine the correction matrices³. Linear or nonlinear color correction functions are applied to each subspace and the transform matrices are optimized in individual subspace.

Color Reproduction System Model

Fig. 1 shows the basic color reproduction system model. An input color scanner is modelled as a forward transformer from input tristimulus value T to signal X , while an output printer also works as forward transformer from the drive signal Y to tristimulus value T . In the color management system, the scanner signal $X=[R, G, B]^t$ is calibrated to carry the correct tristimulus value $T=[X, Y, Z]^t$ by placing its inverse transformer from X to T behind the input device as follows.

$$T = \Phi_{IN}^{-1}(X) \cong M_{SCAN} f_S(X) \quad (1)$$

As well, the color corrector placed in front of printer also works as the inverse transformer from the target tristimulus value T to printer drive signal $Y=[C, M, Y]^t$ as

$$Y = \Phi_{OUT}^{-1}(T) \cong M_{PRNT} f_P(D) \quad (2)$$

Here, the inverse transforms $\Phi_{IN}^{-1}(X)$ and $\Phi_{OUT}^{-1}(T)$ are characterized by polynomial expansions $f_S(X)$ and $f_P(D)$ derived from the device input signals.

In the printing subsystem, $f_P(D)$ includes two steps of signal conversions. First, CIE-XYZ tristimulus input T is transformed into CIE-RGB signal X_{RGB} by 3x3 linear matrix M_{RGB} as

$$X_{RGB} = [R, G, B]^t = M_{RGB} T \quad (3)$$

Next, X_{RGB} is converted into logarithmic density signal D_{RGB} by

$$D_{RGB} = [-\log_{10} R, -\log_{10} G, -\log_{10} B]^t = [D_R, D_G, D_B]^t \quad (4)$$

The matrices M_{SCAN} and M_{PRNT} are optimized to minimize the approximation errors in Eq. (1) and Eq. (2) by the method of least squares.

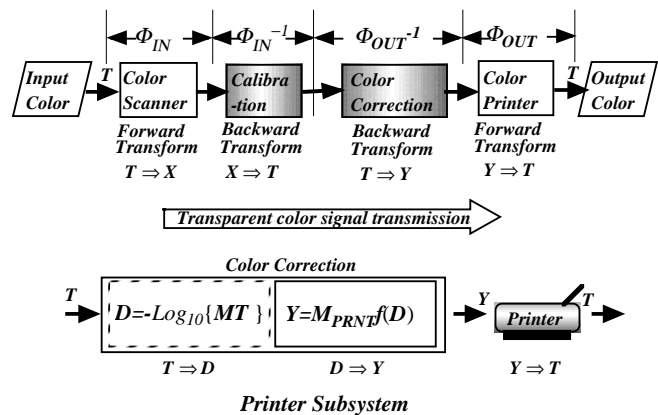


Fig.1 Basic system model

Subspace Models

In the simple color matching system, single matrices M_{SCAN} in scanner and M_{PRNT} in printer are uniformly applied to correct all of the pixels. A most simple way is to divide the entire space into tri-linear boxes with constant volume as shown in Fig.2, where each subspace includes uneven number of color samples. The smaller is the volume of subspace, the higher the color matching accuracy. However, as the number of partitions increases in the conventional tri-linear division, the enough sample number to determine the color correction matrices is not always guaranteed in every cubes. Fig.3 (a), (b), and (c) illustrate the proposed methods. Here all the subspaces are partitioned to include the same number of color samples bounded with nonuniform intervals.

[1] LAB vector division ; M divisions in LAB vector radius r

$$r_j \geq \Delta r_j > r_{j-1} ; j=1 \sim M, \quad r = \{L^{*2} + a^{*2} + b^{*2}\}^{1/2} \quad (5)$$

CIELAB space is divided by 1-D radius r_j to include the constant samples in every spherical cores.

[2] **LC division** ; J divisions in L^* and K divisions in C^*

$$L_j^* \geq \Delta L_j^* \geq L_{j-1}^*, \quad C_k^* \geq \Delta C_k^* \geq C_{k-1}^* ; j=1 \sim J, k=1 \sim K$$

$$C^* = \{a^{*2} + b^{*2}\}^{1/2} \quad (6)$$

CIELAB space is partitioned into totally $M=J \times K$ subspaces along the 2-D luminance-chrominance (LC) axes to include the constant samples in every subspace divided by ΔL_j and ΔC_k^* .

[3] **Polar division** ; J divisions in hue angle and K divisions in LAB vector radius r

$$\theta_j \geq \Delta \theta_j \geq \theta_{j-1} ; j=1 \sim J, \quad \theta = \tan^{-1}(b^*/a^*)$$

$$r_k \geq \Delta r_k \geq r_{k-1} ; k=1 \sim K \quad (7)$$

CIELAB space is partitioned into totally $M=J \times K$ subspaces along the 2-D polar axes to include the constant samples in every subspace surrounded by sector angle $\Delta \theta_j$ and radius Δr_k .

Calibration for Scanner

In the calibration of scanner, IT8/7.2 standard color targets are used as inputs. Here, the XYZ tristimulus values $T_n = [X_n, Y_n, Z_n]^t$ for $n=1 \sim N=256$ color chips are measured by spectro-colorimeter as original test targets. Thus the number of samples included in each subspace is set as

$$Q = N/M = \text{constant} \quad (8)$$

The boundaries between subspaces are determined for each subspace to include Q samples inside.

Letting the color scanner RGB signals be X_q^m ($q=1 \sim Q$, $m=1 \sim M$) corresponding to the input XYZ tristimulus values T_q^m for the m -th subspace, the calibration is performed by the following mathematical transformation.

$$\hat{T}_q^m = M_S^m f_s(X_q^m) = T_q^m \quad (9)$$

Here the scanner signal X_q^m is transformed to be matched to T_q^m by a polynomial expansion $f_s(\text{arg})$ and the coefficient matrix M_{SCAN}^m in Eq.(1) is determined to be partitioned into $\{M_S^m\}$ for individual subspace $m=1 \sim M$.

The matrix M_S^m is optimized so as to minimize the mean square error between the original tristimulus value T_q^m and the approximation \hat{T}_q^m

$$e^2 = \frac{1}{Q} \sum_{q=1}^Q \{ \|T_q^m - \hat{T}_q^m\|^2 \} = \frac{1}{Q} \sum_{q=1}^Q \{ \|T_q^m - M_S^m f_s(X_q^m)\|^2 \} \quad (10)$$

Thus the solution is given by

$$M_S^m = [T_Q^m f_s^t(X_Q^m)] [f_s(X_Q^m) f_s^t(X_Q^m)]^{-1} \quad (11)$$

where, T_Q^m denotes the tristimulus matrix of Q samples in m -th subspace.

$$T_Q^m = \begin{bmatrix} X_1^m, X_2^m, \dots, X_Q^m \\ Y_1^m, Y_2^m, \dots, Y_Q^m \\ Z_1^m, Z_2^m, \dots, Z_Q^m \end{bmatrix} \quad (12)$$

As well, X_Q^m denotes the scanner signal matrix of Q samples in m -th subspace.

$$X_Q^m = \begin{bmatrix} R_1^m, R_2^m, \dots, R_Q^m \\ G_1^m, G_2^m, \dots, G_Q^m \\ B_1^m, B_2^m, \dots, B_Q^m \end{bmatrix} \quad (13)$$

and $f_s(X_Q^m)$ represents the scanner signal matrix expanded by polynomials of Q samples in the same m -th subspace. For example, in the case of 2nd order polynomials, it is given by 10 terms $\times Q$ samples matrix as follows.

$$f_s(X_Q^m) = \begin{bmatrix} R_1^m, R_2^m, \dots, R_Q^m \\ G_1^m, G_2^m, \dots, G_Q^m \\ B_1^m, B_2^m, \dots, B_Q^m \\ (R_1^m)^2, (R_2^m)^2, \dots, (R_Q^m)^2 \\ (G_1^m)^2, (G_2^m)^2, \dots, (G_Q^m)^2 \\ (B_1^m)^2, (B_2^m)^2, \dots, (B_Q^m)^2 \\ (R_1^m G_1^m), (R_2^m G_2^m), \dots, (R_Q^m G_Q^m) \\ (G_1^m B_1^m), (G_2^m B_2^m), \dots, (G_Q^m B_Q^m) \\ (B_1^m R_1^m), (B_2^m R_2^m), \dots, (B_Q^m R_Q^m) \\ 1, 1, \dots, 1 \end{bmatrix} \quad (14)$$

Color Correction for Printer

The inverse transform $\Phi_{OUT}^{-1}(T)$ in printer is known as "color masking" to remove the cross talks in colorants. The forward transform of printer is characterized by measuring the tristimulus values $T^m = [X^m, Y^m, Z^m]^t$ of printed color patches for drive signal $Y_q^m = [C_q^m, M_q^m, Y_q^m]^t$ as

$$T_q^m = \Phi_P^m(Y_q^m) \quad (15)$$

Here, the $N=512$ color patches are printed and their tristimulus values $T_n = [X_n, Y_n, Z_n]^t$; $n=1 \sim N$ are measured. Then $\{T_n\}$ are partitioned into M sets of $\{T_q^m\}$, each including $Q=N/M$ samples for $q=1 \sim Q$ in $m=1 \sim M$ subspaces.

First, the measured tristimulus value T_q^m is converted into logarithmic density signal D_q^m corresponding to the CMY drive signal as given in Eq. (3) and Eq. (4). Then, the inverse transform from T_q^m to Y_q^m is approximated by polynomial expansion. The coefficient matrix M_P^m is optimized to minimize the mean square error between the drive signal Y_q^m and its approximation \hat{Y}_q^m , which is given by

$$M_P^m = [Y_Q^m f_P^t(D_Q^m)] [f_P(D_Q^m) f_P^t(D_Q^m)]^{-1} \quad (16)$$

$$D_Q^m = \begin{bmatrix} D_{R1}^m, D_{R2}^m, \dots, D_{RQ}^m \\ D_{G1}^m, D_{G2}^m, \dots, D_{GQ}^m \\ D_{B1}^m, D_{B2}^m, \dots, D_{BQ}^m \end{bmatrix} \quad (17)$$

$$f_P(D_Q^m) = \begin{bmatrix} D_{R1}^m, D_{R2}^m, \dots, D_{RQ}^m \\ D_{G1}^m, D_{G2}^m, \dots, D_{GQ}^m \\ D_{B1}^m, D_{B2}^m, \dots, D_{BQ}^m \\ (D_{R1}^m)^2, (D_{R2}^m)^2, \dots, (D_{RQ}^m)^2 \\ (D_{G1}^m)^2, (D_{G2}^m)^2, \dots, (D_{GQ}^m)^2 \\ (D_{B1}^m)^2, (D_{B2}^m)^2, \dots, (D_{BQ}^m)^2 \\ (D_{R1}^m D_{G1}^m), (D_{R2}^m D_{G2}^m), \dots, (D_{RQ}^m D_{GQ}^m) \\ (D_{G1}^m D_{B1}^m), (D_{G2}^m D_{B2}^m), \dots, (D_{GQ}^m D_{BQ}^m) \\ (D_{B1}^m D_{R1}^m), (D_{B2}^m D_{R2}^m), \dots, (D_{BQ}^m D_{RQ}^m) \\ 1, 1, \dots, 1 \end{bmatrix} \quad (18)$$

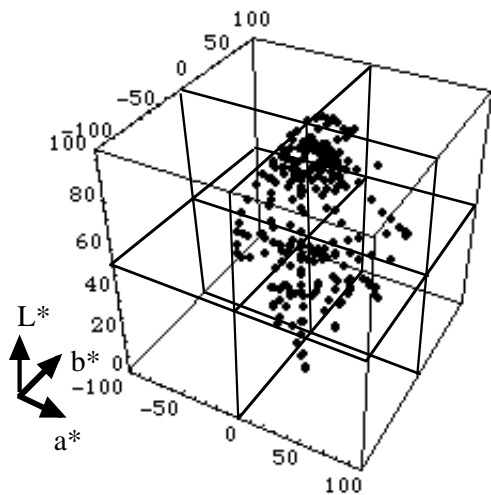
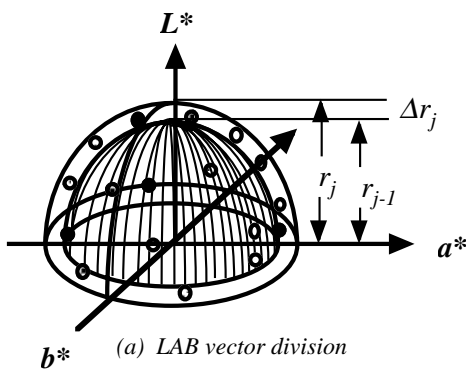
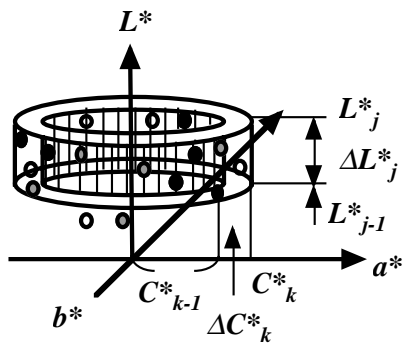


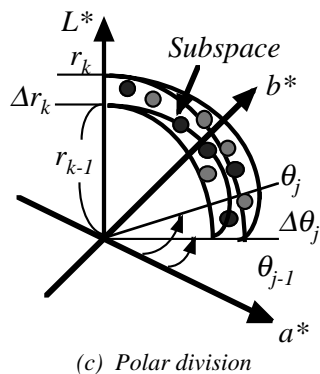
Fig.2 Uniform tri-linear division



(a) LAB vector division



(b) LC division



(c) Polar division

Fig.3 Division methods into subspaces

Experimental Results

The subspace models have been tested on a flat bed scanner and an inkjet printer. $N=256$ color chips in IT8/7.2 standard chart were used for scanner calibration and $N=8^3=512$ color patches were generated on the inkjet printer driven by cmy signals $Y_i=[C_i, M_i, Y_i]^t$ and their tristimulus values $T_o=[X_o, Y_o, Z_o]^t$ were measured by spectrophotometer. Thus, the matrices in printer are calculated by data set $\{Y_i, T_o\}_{i,o=1-512}$.

Fig. 4 shows the calibration errors $\Delta E_{ab}^*(rms)$ for flat bed scanner in case of $M=8$. In all cases, the calibration accuracy has been improved for the higher order polynomials. In order to apply the polynomials with P terms, every subspace should include at least $Q \geq P$ samples. However, it was impossible for uniform tri-linear division to apply 3rd order matrix with $P=20$ in $M=8$, because of $Q < P$. Moreover 2nd order matrix did not give any credit to linear matrix. This may be caused by the uneven sample numbers between the subspaces. On the other hand, proposed division methods resulted in the dramatic improvements in calibration errors. The rms errors by 2nd order matrix in $M=8$, were $\Delta E_{ab}^*(rms)=0.90, 0.75,$ and 0.77 for **LAB vector division**, **LC division**, and **Polar division** respectively. These errors have been further more improved to $\Delta E_{ab}^*(rms)=0.47, 0.35,$ and 0.39 for the use of 3rd order terms. Fig. 5 shows the best result in $\Delta E_{ab}^*(rms)=0.35$ with calibrated IT8/7.2 color map in a^*-b^* plane.

Fig.6 shows the results for inkjet printer in case of $M=8$. The correction matrices are optimized by using the printed color patches as trained targets. Here $\Delta E_{ab}^*(rms)$ is estimated for $N=512$ non-trained color targets generated by a different combination of *CMYs*. Roughly speaking, the color corrections worked very well for non-trained targets as well as trained targets with almost the same accuracy. As clearly shown, the subspace division methods resulted in higher precision color matching than the conventional single matrix method without division. In general, ΔE_{ab}^* is extremely reduced by higher order matrices. However, in the uniform tri-linear division, the best result was given by 2nd order correction, while $\Delta E_{ab}^*(rms)$ increased for 3rd order correction. This may be caused by the same reason as scanner due to uneven color sample numbers. The best correction for trained targets was obtained by LAB vector division with 3rd order polynomials, resulting in $\Delta E_{ab}^*(rms) \approx 1.5$. In the correction for non-trained targets, the best result was obtained by **LC division** with 3rd order polynomials, resulting in $\Delta E_{ab}^*(rms) \approx 2.1$. **Polar division** showed stable and excellent results in both trained and non-trained estimations. It resulted in $\Delta E_{ab}^*(rms) \approx 2.7$ by 2nd order and ≈ 2.2 by 3rd order correction for trained targets and $\Delta E_{ab}^*(rms) \approx 2.6$ by 2nd order and ≈ 2.4 by 3rd order correction for non-trained target. Fig.7 shows an example of reproduced color targets in a^*-b^* plane after printer correction.

Fig.8 illustrates how the correction error decreases as the division number M increases in case of **Polar division** for trained targets. The rms errors are reduced monotonously with the division number M . The color differences are going to approaching to around $\Delta E_{ab}^*(rms) \approx 1.5$ as the M increases.

Discussion and Conclusion

The high precision color calibrations for input/output devices have been approached by the optimization in subdivided color spaces. Nonuniform division to subspaces, including the equal number of color samples in each, makes it possible to use the higher order of nonlinear matrices. In the application to scanner, the calibration accuracy could be

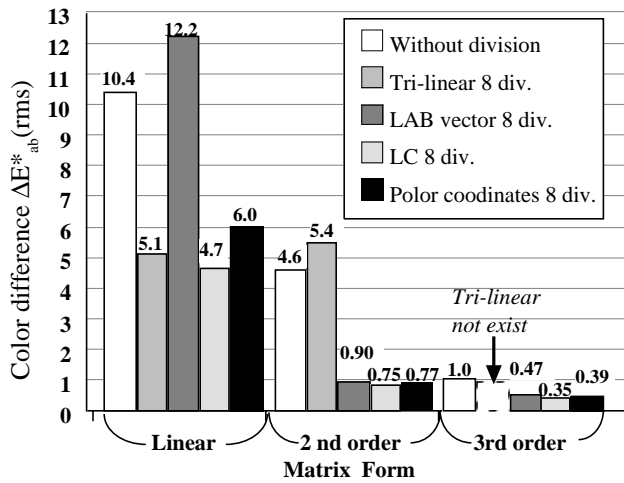


Fig.4 Calibration errors in flat bed PC scanner

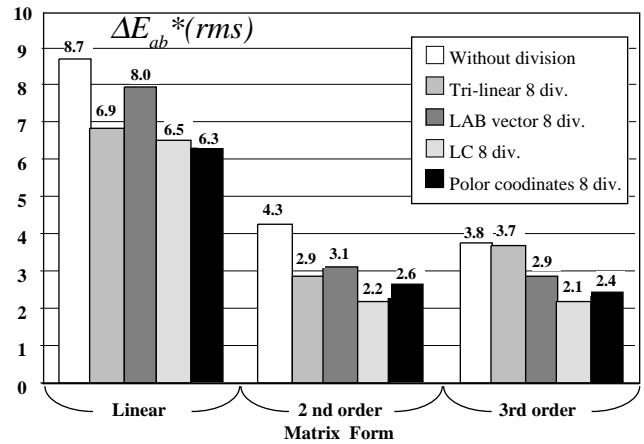
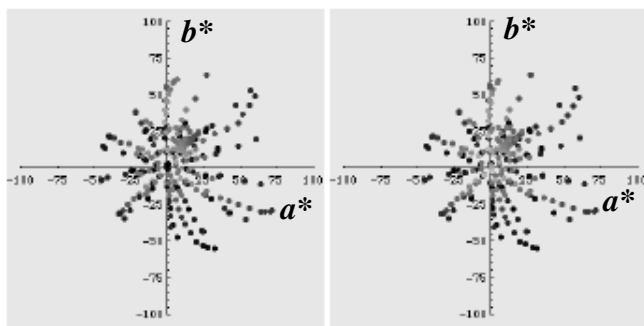
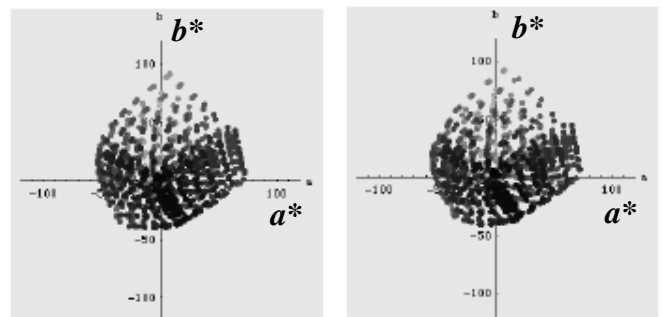


Fig.6 Color correction errors in inkjet printer (non-trained target)



(a) Original (b) LC M=8 div., 3rd order : $\Delta E_{ab}^*(rms) = 0.35$

Fig.5 Calibrated IT8/7.2 target in flat bed PC scanner



(a) Original (b) Corrected by LC 8 div. 2nd order : $\Delta E_{ab}^*(rms) = 2.2$

Fig.7 Color map of corrected chips in inkjet printer

dramatically improved by operating the nonlinear matrices with 2nd order or 3rd order polynomials optimized in each subspace. The rms color differences as well as maximum color differences could be reduced to about 1/5 as compared with conventional methods, reaching to $\Delta E_{ab}^*(rms) \approx 0.35$ and $\Delta E_{ab}^*(max) \approx 1.6$ for scanner. These values may be comparable to the colorimetric measurement errors.

In the application to printer color correction, the proposed method resulted in high precision reproductions around $\Delta E_{ab}^*(rms) \approx 2$ for inkjet printer. 1-D LAB vector division worked well resulting in $\Delta E_{ab}^*(rms) \approx 1.5$ with 3rd order matrix. 2-D Polar division worked stable for both trained and non-trained targets. It approached to $\Delta E_{ab}^*(rms) \approx 1.5$ for trained targets. LC division with 3rd order matrix resulted in the highest reproduction with $\Delta E_{ab}^*(rms) \approx 2.1$ for non-trained targets. These values are almost approaching to the mechanical stability around $\Delta E_{ab}^*(rms) \approx 1.0$ in low-end use.

The gamut compression process is not included in this paper but necessary for the inputs outside the printer gamut and is under development.

References

1. H.Kotera, *JIEEEJ*, 14,5, 298-307(1985)
2. H.Ikegami, *Proc. OELASE'89, SPIE*, 1075-1105(1989)
3. P. C. Hung, *Proc. SPIE*, 1448, 164-174(1991)
4. K.Kanamori and H.kotera, *J. IS&T*, 36, 1, 73-80(1992)
5. R. Balasubramainen, *Proc. 2nd CIC*, 62-65(1994)
6. H.Haneishi et al, *Proc. 3rd CIC*, 106-108(1995)
7. T. Johnson, *Displays*, 16,4,183-192(1996)

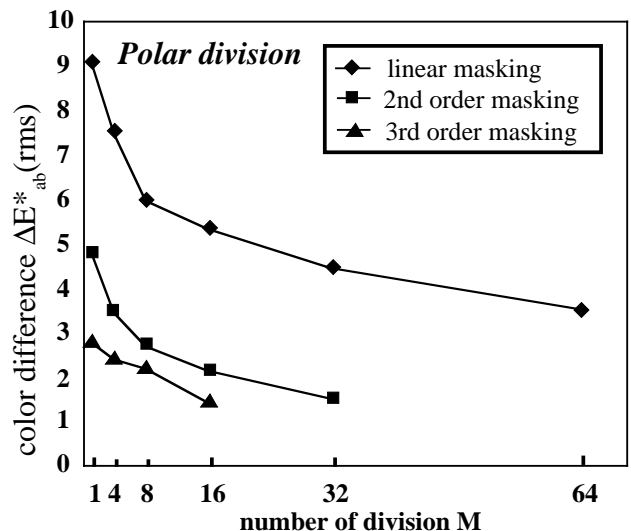


Fig.8 Color correction errors in inkjet printer vs M

8. T. Johnson, *Displays*, 16,4,193-202(1996)
9. A.Ishige, C. Hung-Shing, and H.Kotera, *Proc. PPIC/JH'98P58*, 375-378(1998)